Burning velocity measurements of fluoropropanes by the spherical-vessel method

Kenji Takizawa *, Akifumi Takahashi, Kazuaki Tokuhashi, Shigeo Kondo, Akira Sekiya

National Institute of Advanced Industrial Science and Technology (AIST), Central 5, 1-1-1 Higashi, Tsukuba, Ibaraki 305-8565, Japan

ARTICLE INFO

ABSTRACT

Burning velocity measurements of six types of fluoropropanes including structural isomers were carried out in order to understand the flammability of hydrofluorocarbons (HFC). The burning velocity (S_u) was determined by applying a spherical flame model to the pressure rise during combustion, which was measured at room temperature and at initial pressures of 80–107 kPa over a wide range of HFC/air concentrations. The maximum S_u of 1-fluoropropane (HFC-281fa), 2-fluoropropane (HFC-281ea), 1,3-difluoropropane (HFC-272fa), 2,2-difluoropropane (HFC-272ca), 1,2,3-trifluoropropane (HFC-263ea), and 1,1,1-trifluoropropane (HFC-263fb) was 35.0, 31.8, 31.9, 21.2, 25.7, and 14.5 cm s^{-1}, respectively. Note that the maximum S_u of HFC-263ea was appreciably higher than that of HFC-272ca, which shows the importance of the F-atom distribution, as well as of the F/H ratio in the HFC molecule. The results of equilibrium calculation for these HFCs showed that S_u is positively correlated with the flame temperature and the concentrations of the active chain carriers H and OH in the flame. We conducted a trial to interpret the magnitude of S_u by means of the effects of substituents for C$_1$–C$_3$ HFCs. As a result, it has been found that the order of inhibition efficiency for S_u decreases in the order of CF$_3$ > CF$_2$ > CF.

© 2008 Elsevier B.V. All rights reserved.

1. Introduction

A wide variety of hydrofluorocarbons (HFCs) are currently used as refrigerants, foam-blowing agents and cleaning solvents because of their generally useful properties, such as high efficiency, low toxicity, and short atmospheric lifetime. The latter property is mainly due to the reactivity between OH radicals and H atoms present in the molecule. On the other hand, a number of HFCs are flammable in air because of the presence of H. In practice, non-flammable HFCs are preferably used; otherwise flammable HFCs are mixed with less reactive compounds to decrease flammability. However, considering the expanding number of HFCs and HFC-blended products presently under development, appropriate and reliable risk assessment becomes important to prevent and control fire hazards. For this purpose, a number of flammability characteristics have been investigated, e.g., burning velocity (S_u), flammability limits, heat of combustion (H_c), etc. Among these, S_u is a promising parameter for describing the rate of combustion reactions, and hence the severity of fire hazards. To understand behavior of S_u of various types of HFCs, it is necessary to accumulate the S_u data of HFCs by either direct measurements or reliable estimation methods. For hydrocarbons, Davis and Law [1] compiled experimental S_u data for C$_1$–C$_8$ compounds with various structures including saturated, unsaturated, and cyclic species. According to their results, methyl substitution for the H atom reduces S_u, whereas an unsaturated structure causes S_u to increase. The values of S_u for normal alkanes except CH$_4$ were very comparable, which could be attributed mainly to similarity in the oxidation kinetics. For HFCs, however, experimental S_u data to date have been limited to flammable C$_1$ and C$_2$ fluoroalkanes [2–5] and CH$_4$/air flames inhibited by nonflammable C$_1$–C$_3$ fluorocarbons [6,7]. We have recently studied the S_u for small alkanes and all flammable C$_1$ and C$_2$ fluoroalkanes [3,4], most of which are used as refrigerants, by employing the spherical vessel (SV) and schlieren photography (SP) methods. The SV method, using a closed vessel with central ignition, provides the S_u data from measurement of the pressure–time profile during combustion by assuming a spherical flame propagation model. The observed maximum S_u for the C$_1$ and C$_2$ fluoroalkanes ranged widely, from 6.7 cm s^{-1} for difluoromethane (HFC-32) to 38.3 cm s^{-1} for fluoroethane (HFC-161). We suggested that the S_u of HFCs is strongly dependent on the ratio of F to H atoms in the molecule, probably because HFCs generate fluoric species that act as inhibitors and stabilize the active chain carriers, H and OH, by producing HF through the combustion process. On the other hand, S_u considerably differed among structural isomers, despite the same F/H ratio in the molecule. For example, the maximum S_u for 1,1,1-trifluoroethane (HFC-143a, 7.1 cm s^{-1}) was roughly half that of 1,1,2-trifluoroethane (HFC-143, 13.1 cm s^{-1}). Thus, the difference in S_u is not adequately explained solely in terms of F-substitution in the

molecule. In order to evaluate S_u the effects of the molecular structure should also be taken into consideration.

In this study we extend the tested compounds to the C_3 series in order to understand the factors that determine the magnitude of S_u of various HFCs. Since fluoropropanes have a number of structural isomers, they are good subjects for elucidating the structural effects of HFCs on their respective S_u. There have been few reports on S_u measurements of C_3 HFCs. Linteris et al. [7] published burning velocity measurements of CH_4/air mixtures inhibited by C_3F_8 and CF_3CHFCF_3 as well as several most fluorinated ethanes. Williams et al. [8] compared the S_u data of Ref. [7] with calculations using a kinetic mechanism describing the consumption of these compounds. According to their results [8], the ratios of calculated to experimental S_u were in the range 0.70–1.11. Since such calculations should be based on a considerable number of the relevant elementary reactions, it is necessary to measure detailed time profiles of the concentrations for the relevant chemical species to clarify the primary consumption routes and to obtain global parameters such as S_u. However, there are very few experimental elementary reaction rates and the chemical kinetic mechanism has not been developed for flammable C_3 HFCs, compared with C_1 and C_2 compounds [9]. Taking these facts into consideration we try to express the value of S_u by using total molecular structure–flammability relationships. In this study we measured S_u for six fluoropropanes, namely 1-fluoropropane (HFC-281fa), 2-fluoropropane (HFC-281ea), 1,3-difluoropropane (HFC-272fa), 2,2-difluoropropane (HFC-272ca), 1,2,3-trifluoropropane (HFC-263ea), and 1,1,1-trifluoropropane (HFC-263fb), by the same SV method as previously applied to C_1 and C_2 fluoroalkanes [3,4]. The similarity of the test method allowed us to compare quantitatively the data obtained for the fluoropropanes with those previously determined for the alkanes and C_1 and C_2 fluoroalkanes [3,4]. The rationale was that by comparing S_u data obtained by the same method we may be able to clarify what are the characteristic molecular structures that control the magnitude of this parameter and improve techniques for its estimation. Then we tried to determine S_u by applying an analytical evaluation to these compounds with various molecular structures.

2. Results and discussion

2.1. Burning velocity measurements

In the SV method, S_u was experimentally obtained as a function of temperature (T) and pressure (P), because the unburned region in the closed vessel was compressed adiabatically while the flame propagated outwards [3]. The S_u was fitted to the following empirical equation:

$$S_u = S_{u0}\left(\frac{T}{T_s}\right)^{\alpha}\left(\frac{P}{P_s}\right)^{\beta}. \tag{1}$$

Here $T_s = 298$ K, $P_s = 760$ Torr (1 Torr = 133 Pa), S_{u0} is the burning velocity at T_s and P_s, and α and β are the fitting parameters describing the powers of the temperature and pressure dependence, respectively. For each concentration we took measurements at three initial pressure (P_0) values, namely 600, 700, and 800 Torr and S_{u0} was determined by applying Eq. (1) to the results. This technique is based on the assumption that the flame front is smooth and remains spherical during propagation. The spherical flame assumption is considered valid as long as the flame propagation is rapid enough to be negligibly affected by the effect of buoyancy. We confirmed that the SV method was consequently applicable when S_u was higher than approximately 5 cm s^{-1} [3]. In the present study, since S_u for these fluoropropanes was relatively high, we presume that the flame fronts propagated spherically. On the other hand, it was found that the flame surfaces of these fluoropropanes were not always regarded as smooth. Fig. 1a–d shows the schlieren images of flames for HFC-281fa at various sample/air concentrations. In these figures the radii (r_f) of these four flames are nearly equal. The small dimples observed in the horizontal direction were due to a cooling effect of the electrodes.
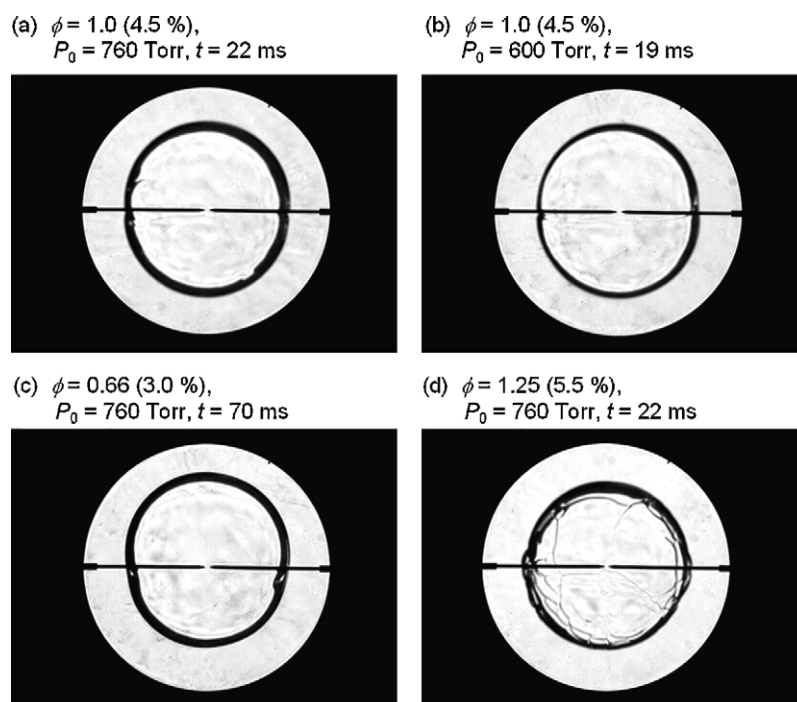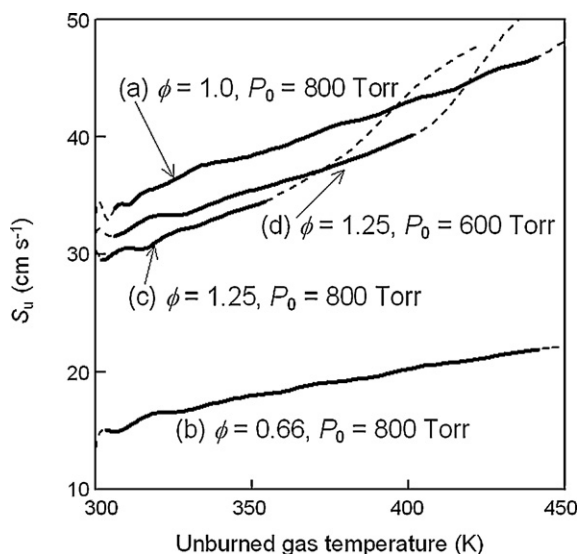

(a) $\phi = 1.0$ (4.5 %), $P_0 = 760$ Torr, $t = 22$ ms

(b) $\phi = 1.0$ (4.5 %), $P_0 = 600$ Torr, $t = 19$ ms

(c) $\phi = 0.66$ (3.0 %), $P_0 = 760$ Torr, $t = 70$ ms

(d) $\phi = 1.25$ (5.5 %), $P_0 = 760$ Torr, $t = 22$ ms

Fig. 1. Schlieren images for the flames of HFC-281fa/air mixtures. The value in parentheses of each image denotes HFC-281fa/air concentration (*Note*: ϕ, the equivalence ratio is defined later on in the text).
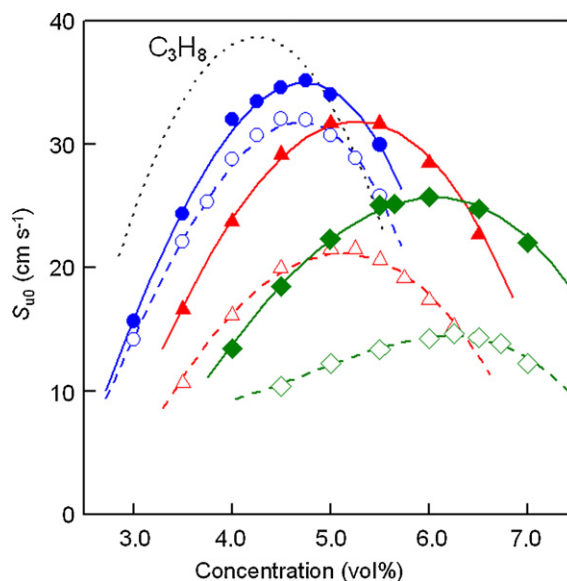
Fig. 2. S_u curves for HFC-281fa/air mixture. The bold parts of these curves are used for the determination of S_{u0} using Eq. (1) (*Note*: Please see our note on the meaning of ϕ in Fig. 1).

Fig. 3. S_{u0} for the HFC/air mixtures. HFC-281fa (●); HFC-281ea (○); HFC-272fa (▲); HFC-272ca (△); HFC-263ea (◆); and HFC-263fb (◇). The curves present values obtained using Eq. (2).

For the stoichiometric flames (Fig. 1a and b), a few faint wrinkles were observed as the flame propagated outwards. Comparison of the flames between P_0 = 760 and 600 Torr indicates that the former flame formed wrinkles in the earlier phase of propagation with smaller r_f. For the 'lean' flame (Fig. 1c), such wrinkles were not observed and the flame sphere remained smooth during the whole propagation period. On the other hand, for the 'rich' flame (Fig. 1d), a number of wrinkles appeared from the middle period of propagation and a cellular structure, which is considered to enhance the flammability, was partially formed during propagation. For the other HFCs, similar tendencies were observed for the relationship between the flame shape and the HFC/air equivalence ratio. If the data obtained under such cellular flames were taken into the present fitting procedures using Eq. (1), the obtained S_{u0} would deviate from the values of the laminar flames. From the plots of the experimental S_u as a function of the unburned gas temperature obtained from the pressure–time profiles (Fig. 2), we observed that S_u increased regularly with increasing unburned gas temperature for the low and stoichiometric concentrations (Fig. 2a and b), but for the higher concentrations, S_u increased drastically (Fig. 2c and d), from the middle of the temperature range. The irregular change in the S_u curves may correspond to the onset of the cellular structure due to instabilities. This phenomenon seems to be dependent not only on the concentration but also on the initial pressure of the gas mixture (see the curves in Fig. 2c and d). To avoid the overestimation of S_{u0} due to irregular curvatures, we used only the regular parts of the S_u curves (the bold lines in Fig. 2). Fig. 3 shows the measured S_{u0} values as a function of HFC/air concentration in volume percent for C_3 HFCs along with C_3H_8. The equivalence ratio (ϕ) was determined on the basis of the following overall reaction:

$$C_nH_{2n-m+2}F_m + \frac{3n-m+1}{2}O_2 \rightarrow mHF + nCO_2 + (n-m+1)H_2O \qquad (R1)$$
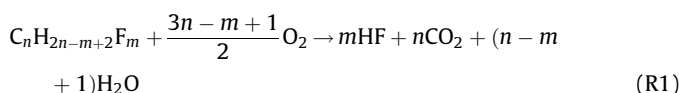
Since S_{u0}, α, and β in Eq. (1) depend on ϕ, we performed a nonlinear least-squares fitting of all the data measured at various concentrations using the following equations:

$$S_{u0} = S_{u0,max} + s_1(\phi - \phi_{max})^2 + s_2(\phi - \phi_{max})^3, \qquad (2)$$

$$\alpha = a_1 + a_2(\phi - 1), \qquad (3)$$

$$\beta = b_1 + b_2(\phi - 1). \qquad (4)$$

Here $S_{u0,max}$, s_1, s_2, ϕ_{max}, a_1, a_2, b_1, and b_2 are the fitting parameters. $S_{u0,max}$ is the maximum burning velocity at T_s, P_s, and ϕ_{max}; a_1 and b_1 are the values of α and β, respectively, at ϕ = 1. The cubic form of Eq. (2) represents the asymmetric nature of the dependence of S_{u0} on ϕ. The resulting values of the parameters in Eqs. (2)–(4) are listed in Table 1. For ϕ_{max}, a_1, and b_1, which represent dependence of S_u on sample concentration, temperature, and pressure, respectively, the obtained values were similar among these six compounds. In Fig. 3, the symbols denote the observed values from the measurements for each concentration, and the curves represent Eq. (2) obtained by the above procedure. All the symbols did not exhibit discrepancy from the S_{u0} curves, which indicates that the obtained S_{u0} was valid throughout the entire range of concentrations without any changes being caused by flame discontinuity at the rich conditions. From these curves we obtained the maximum burning velocities $S_{u0,max}$ and the corresponding equivalence ratios ϕ_{max}.

2.2. Comparison of flammability properties of HFCs

For C_1–C_3 alkanes and HFCs, the observed $S_{u0,max}$ and the relevant properties are summarized in Table 2.

In general the burning velocity of HFC is likely to decrease with increasing the F-substitution rate, $n_F/(n_H + n_F)$, as listed in Table 1. The higher the F-substitution rate, the more fluoric species and the less active chain carriers (especially H and OH) are expected to exist in the flame. Comparing the three pairs of the structural isomers of this study, the S_u results for the two HFC-281 isomers are fairly comparable, whereas those for HFC-272 and HFC-263 isomers are appreciably different, despite the same F-substitution rate of the isomer. Roughly speaking, if F atoms are more widely distributed in isomer molecules, the value of S_u increases. Furthermore, comparison of the $S_{u0,max}$ value between HFC-281ea and HFC-272fa and between HFC-272ca and HFC-263ea shows that in each of these pairs, the first molecule has a lower $S_{u0,max}$ than the second, though the former has a lower F-

Table 1
Burning velocities of C$_3$ HFCs

Compound	Chemical formula	S_{u0} (cm s^{-1})				α		β	
		$S_{u0,max}$	s_1	s_2	ϕ_{max}	a_1	a_2	b_1	b_2
HFC-281fa	CH$_3$CH$_2$CH$_2$F	35.0	−142.0	−55.8	1.06	1.82	−1.50	−0.26	0.36
HFC-281ea	CH$_3$CHFCH$_3$	31.8	−147.6	−87.4	1.06	1.74	−1.17	−0.25	0.25
HFC-272fa	CH$_2$FCH$_2$CH$_2$F	31.9	−117.0	−15.1	1.06	1.69	−0.84	−0.23	0.25
HFC-272ca	CH$_3$CF$_2$CH$_3$	21.2	−91.2	−6.4	1.03	1.89	−1.35	−0.27	0.24
HFC-263ea	CH$_2$FCHFCH$_2$F	25.7	−95.1	−32.9	1.07	1.75	−0.63	−0.22	0.09
HFC-263fb	CH$_3$CH$_2$CF$_3$	14.5	−64.0	−81.2	1.10	1.96	−1.45	−0.23	0.26

α and β are coefficients for temperature and pressure dependence for Eq. (1); $S_{u0,max}$, s_1, s_2, ϕ_{max}, a_1, a_2, b_1, and b_2 are the fitting parameters of Eqs. (2)–(4).

Table 2
Flammability properties of C$_1$–C$_3$ alkanes and HFCs

Compound	Chemical formula	$n_F/(n_H + n_F)$	$S_{u0,max(exp)}$ (cm s^{-1})	$S_{u0,max(pred)}$ (cm s^{-1})	H_c (kJ mol^{-1})	C_{st} (vol%)	LFL (vol%)	UFL (vol%)	T_{ad} (K)
Methane	CH$_4$	0	36.5	39.6	802[a]	9.50	4.9[c]	15.8[c]	2587
HFC-41	CH$_3$F	0.25	28.3	29.9	675[a]	12.28	7.1[c]	19.9[c]	2650
HFC-32	CH$_2$F$_2$	0.5	6.7	6.5	486[a]	17.36	13.5[c]	27.5[c]	2592
Ethane	C$_2$H$_6$	0	40.9	36.2	1428[a]	5.66	3.0[c]	12.5[c]	2623
HFC-161	CH$_3$CH$_2$F	0.167	38.3	31.3	1280[a]	6.54	3.15[b]	17.5[b]	2639
HFC-152	CH$_2$FCH$_2$F	0.333	30.1	26.4	1140[a]	7.75	4.15[b]	19.0[b]	2669
HFC-152a	CH$_3$CHF$_2$	0.333	23.6	19.6	1073[a]	7.75	4.35[c]	17.5[c]	2590
HFC-143	CH$_2$FCHF$_2$	0.5	13.1	14.8	940[a]	9.50	6.2[c]	22.6[c]	2629
HFC-143a	CH$_3$CF$_3$	0.5	7.1	6.8	859[a]	9.50	7.4[c]	17.0[c]	2509
Propane	C$_3$H$_8$	0	38.7	36.2	2043[b]	4.03	2.1[c]	9.5[c]	2631
HFC-281fa	CH$_3$CH$_2$CH$_2$F	0.125	35.0	32.9	1889[b]	4.46	2.38[b]	10.2[b]	2640
HFC-281ea	CH$_3$CHFCH$_3$	0.125	31.8	32.9	1867[b]	4.46	2.38[b]	10.0[b]	2625
HFC-272fa	CH$_2$FCH$_2$CH$_2$F	0.25	31.9	29.7	1748[b]	4.99			2654
HFC-272ca	CH$_3$CF$_2$CH$_3$	0.25	21.2	25.1	1653[b]	4.99			2589
HFC-263ea	CH$_2$FCHFCH$_2$F	0.375	25.7	26.4	1584[b]	5.66			2665
HFC-263fb	CH$_3$CH$_2$CF$_3$	0.375	14.5	16.6	1454[b]	5.66	3.6[b]	12.4[b]	2553

$n_F/(n_H + n_F)$, F-substitution rate, where n_H and n_F are the numbers of H and F atoms in the molecule; $S_{u0,max(exp)}$, observed maximum burning velocity; $S_{u0,max(pred)}$, maximum burning velocity estimated from Eq. (5); H_c, heat of combustion; C_{st}, stoichiometric concentration; LFL and UFL, lower and upper flammability limit, which were observed by an ASHRAE-type method [10,12]; T_{ad}, adiabatic flame temperature for constant-volume combustion at $\phi = 1$, $T_0 = 298$ K and $P_0 = 760$ Torr.
 [a] From the enthalpy of formation for HFCs and the products in Ref. [9].
  [b] From theoretical calculation of the heat of formation in Ref. [11] and the combustion reaction on the basis of reaction (R1).
  [c] Ref. [12].

substitution rate. The perfluoroalkyl substituents, i.e., the primary CF$_3$ and secondary CF$_2$, may decrease S_u since the difference in $S_{u0,max}$ is large between the compound with perfluorinated alkyl substitute and its isomer, e.g., HFC-272ca and HFC-272fa, and HFC-263ea and HFC-263fb. Thus, if the distribution of F atoms in the molecule varies, S_u also varies.

Concerning the effect of the active species in the flame, the concentrations of the H, OH, and O on the magnitude of S_u are worth consideration. During the combustion of HFCs, H, OH, and O act as chain carriers of the chain-branching reactions by generating another active species, whereas the F atom is believed to contribute to flame extinction by deactivating an H atom to convert to stable HF, which results in termination of the chain reactions. Therefore, as the concentrations of the chain-carrying species (H, OH, and O) in the HFC flame decreased, the consumption of the HFC and the intermediates became less effective, and as a consequence we expected S_u to decrease. We carried out equilibrium calculations of the stoichiometric HFC flame under constant-volume conditions. Although it is known that concentrations of the chemical species in the reaction zone often reach much higher levels than the equilibrium values, the calculated values of radical concentrations may show a valuable tendency for the following discussion and help us to understand the effectiveness of the combustion reactions of HFCs qualitatively. When S_{u0} at the stoichiometric concentration ($S_{u0,st}$) was low, the mole fractions of H and OH were relatively low (Fig. 4a and b); as the value of $S_{u0,st}$ increased, the mole fractions of H and OH

increased almost linearly. According to the models of CH$_4$/air flames inhibited by fluorocarbons [6,7], the concentration of H in the reaction zone is more significantly related to the burning velocity than that of OH. The results of numerical modeling of the H$_2$/air flames inhibited by CF$_3$CHFCF$_3$ [13] also suggest that the removal of H will have an overall inhibition effect rather than that of OH. From the result of equilibrium calculation, however, it is not clear which concentration is directly correlated to the magnitude of S_u, probably because the equilibrium concentrations of H and OH are attained after the shuffle reactions such as OH + H$_2$ → H$_2$O + H and H + O$_2$ → O + OH. Compared with H and OH, the mole fraction of O atoms (Fig. 4c) seems not to be sensitive to the $S_{u0,st}$ of the corresponding HFCs, probably because O atoms are not directly trapped by F atoms. The mole fraction of F atoms (Fig. 4d) was very low and even at the highest concentration (in HFC-263ea), it only reached a factor of ca. 0.3 of that of H atoms. These observations show that the flames of HFCs with higher S_u values have higher equilibrium concentrations of H and OH, as well as lower F-substitution rates. Also the isomers with a higher concentration of H and OH (HFC-281fa, HFC-272fa, and HFC-263ea) have a higher S_u than their counterparts (HFC-281ea, HFC-272ca, and HFC-263fb). Considering difference in the flame temperature (Table 2), the isomer with a higher T_{ad} has a higher S_u. Difference in T_{ad} seems to be due to difference in the bond energies of the compound. To examine the effect of T_{ad}, we calculated the equilibrium concentrations of the chemical species in the stoichiometric C$_1$–C$_3$ HFC flames at the same flame temperature by changing the
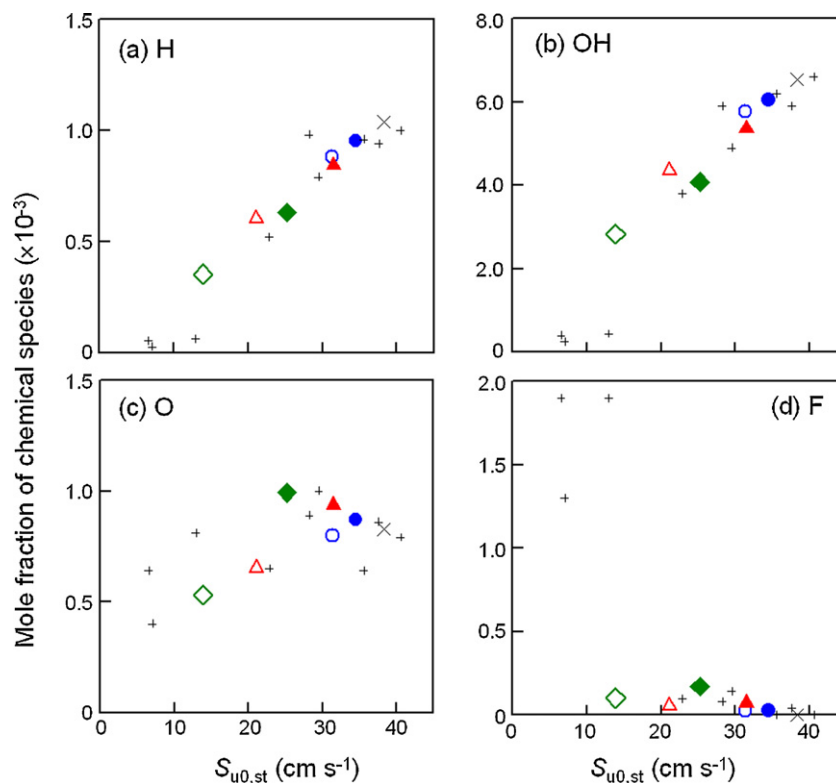
Fig. 4. Calculated equilibrium mole fraction of the chemical species at the adiabatic flame temperature vs. the stoichiometric burning velocity ($S_{u0,st}$) for HFC/air mixtures. HFC-281fa (●); HFC-281ea (○); HFC-272fa (▲); HFC-272ca (△); HFC-263ea (◆); HFC-263fb (◇); C_3H_8 (×); C_1 and C_2 HFCs and alkanes (+) (see also Fig. 6 in Ref. [4]).

initial concentration of inert N_2 under constant HFC/O_2 ratio ($\phi = 1$). Considering the fact the initial composition of HFCs, O_2, and N_2 mixtures was slightly different between the isomers, the calculated concentrations of H, OH, O, and F were very similar between the isomers and the relative differences were at most 7% for the C_2 and C_3 isomers. Such similarity was also obtained by the equilibrium calculations under constant-pressure conditions. This fact indicates that the molecular structural differences between the isomers lead to differences in the flame temperature and may also lead to differences in the reaction kinetics, and hence differences in S_u.

2.3. Analytical evaluation of S_u for C_1–C_3 HFCs

For self-sustaining flame propagation to occur, sufficient energy release and active species to sustain the chain reaction in the flame are required. We consider global parameters of the combustion reaction such as S_u to be intrinsically connected with the molecular structure and expect that S_u can be expressed by an analytical form in terms of various bonds and atomic groups that constitute the molecule. Within the present study, the main structural factors that can affect the S_u are the carbon skeleton (or carbon chain length) and substitution of F atoms for H atoms, i.e., the number and distribution of F atoms. The sum of the contributions of these factors within a molecule might determine S_u. To take these conditions into consideration, a number of structural parameters were introduced in the analysis. The following equation was employed to interpret S_u of C_1–C_3 HFCs

$$S_{u0,max} = p_1(1 + p_2 R_{C_1} + p_3 R_{CF_3} + p_4 R_{CF_2} + p_5 R_{CF}). \qquad (5)$$

Here, p_1–p_5 are coefficients and fitting parameters for the various terms of $S_{u0,max}$ to be determined from our analysis of the observed data. R_{C_1} is the descriptor for whether the molecule is a C_1 compound or not. It is known that the lowest bond dissociation energy, D(C–H), decreases with increasing carbon chain length, e.g., D(C–H) for CH_4, CH_3CH_3, $CH_3C^*H_2CH_3$, and $CH_3C^*H_2CH_2CH_3$ is 104.9, 101.1, 98.6, and 98.2 kcal mol^{-1}, respectively [13]. From this viewpoint it might seem more plausible to express the descriptor as a function of the number of carbon skeletons. However, the D(C–H) decrease is the largest for the first step and the observed $S_{u0,max}$ of these alkanes showed an anomalous order like $CH_4 < C_3H_8 < C_2H_6$ [1–4], in spite of the trend of D(C–H). In order to cope with this situation, we considered that at the first approximation it may only matter whether the molecule is of mono-carbon skeleton ($R_{C_1} = 1$) or not ($R_{C_1} = 0$). R_{CF_3}, R_{CF_2}, and R_{CF}, respectively denote the numbers of CF_3, CF_2, and CF groups in the molecule divided by the number of carbon atoms. These ratios represent the effect of tri-, di-, and mono-substitution of F atoms on $S_{u0,max}$. Note that Eq. (5) does not take into account the number of alkyl groups, hence the distinction of C_2H_6 and C_3H_8, and neither does it distinguish between a primary CH_3 group and a secondary CH_2 group in C_3 compounds, hence HFC-281fa and HFC-281ea. Since the relative difference between the $S_{u0,max}$ of the members of these two pairs of compounds was no more than 10% and the amount of experimental data was so far limited, we tried to reduce the number of parameters in the analysis rather than to distinguish all the compounds by introducing more sophisticated descriptors. Under these conditions we carried out the numerical analysis for the 16 C_1–C_3 compounds (Fig. 5). The predicted values of $S_{u0,max}$ are listed as $S_{u0,max(pred)}$ in Tables 2 and 3 lists the fitting parameters. On the whole, the agreement between the experimental and predicted values was satisfactory, although discrepancies remained for some compounds. The ratios of $S_{u0,max(pred)}$ to the experimentally obtained $S_{u0,max}$, $S_{u0,max(exp)}$, were in the range 0.82–1.19 and the average relative deviation of $S_{u0,max(pred)}$ from $S_{u0,max(exp)}$ was 9.6%. For C_2 compounds, however, most of the
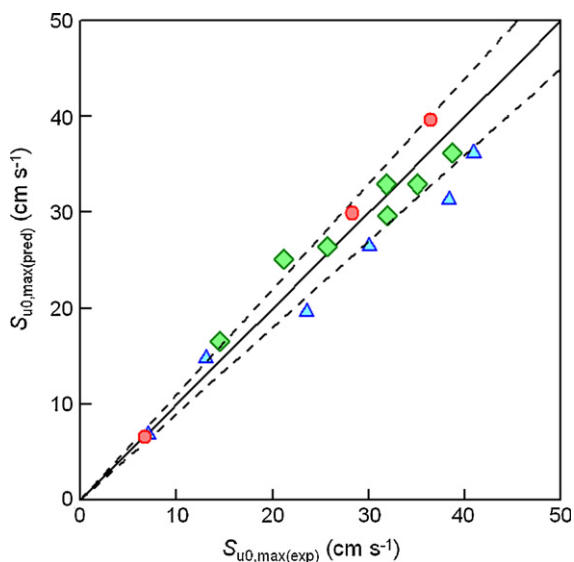
Fig. 5. Comparison of observed and predicted $S_{u0,max}$ for C_1–C_3 HFCs and alkanes. C_1 compound (●); C_2 compound (▲); C_3 compound (◆); solid line, perfect fit; dashed line, factors of $\pm 10\%$ deviation from perfection.

Table 3
The values of the p_i coefficients by the analysis

p_i	Description of structure	Value	Value est. 2[a]
p_1	Main coefficient	36.174	37.753
p_2	C_1 molecule or not	0.096	0.069
p_3	CF_3	−1.627	−1.646
p_4	CF_2	−0.915	−0.895
p_5	CF	−0.269	−0.306

[a] est. 2 excludes HFC-272ca from HFCs in the original estimation.

calculated values were lower than the experimental ones (the triangles in Fig. 5). We attributed this systematic deviation to the introduction of R_{C_1}. We consider improving the estimation by replacing R_{C_1} with another descriptor. For example, the number of C–C bonds relative to the number of C, n_{C-C}/n_C, in the molecule shows an approximately linear inverse correlation with the experimental $D(C-H)$ values of CH_4, C_2H_6, $CH_3C^*H_2CH_3$, and $CH_3C^*H_2CH_2CH_3$ [14]. However, when R_{C_1} was replaced by this descriptor considering the effect of decreasing $D(C-H)$ with carbon chain length, the new coefficient p_2 showed a rather negative value, which results in overestimation of $S_{u0,max}$ for C_1 compounds. The problem was caused by the anomalous ordering of $S_{u0,max}$ for the carbon chain length, as mentioned above, and this problem unfortunately remains unsolved.

Considering the other coefficients of the descriptors in Table 3, the CF_3 structure was found to reduce $S_{u0,max}$, as represented by a relatively large negative coefficient of p_3. The absolute value of p_3 was greater than 1.5 times that of p_4 and much greater than 3 times that of p_5. This is correspondent to the experimental results that HFC-143a and HFC-263fb, which have a CF_3 group, had significantly lower $S_{u0,max}$ values than their isomers, HFC-143 and HFC-263ea. Regarding R_{CF} and R_{CF_2} in Eq. (5), each of them contains two structures, depending on the primary or secondary carbon site. For R_{CF}, a typical case is a primary CH_2F in HFC-281fa and a secondary CHF in HFC-281ea. The structural effects of the two substituents seem similar since the difference in $S_{u0,max}$ between these isomers is less than 10%. For R_{CF_2}, the flammability characteristics of primary CHF_2, which is present in HFC-152a and HFC-143, and the secondary perfluoroalkyl CF_2, present in HFC-272ca, may have

different effects. Comparison of S_u between HFC-272ca and its isomer $CH_3CH_2CHF_2$ (HFC-272fb) would reveal the difference of the structural effects, but we have not found the S_u data for HFC-272fb. Accordingly, we excluded HFC-272ca from the numerical analysis and re-estimated S_u of the other 15 compounds. The resulting parameters are listed as est. 2 in Table 3. The inhibition effect of CF_2, represented as the absolute value of parameter p_4 of est. 2 became slightly smaller than that of the original estimation, which may result from exclusion of the effect of a secondary CF_2, i.e., the secondary CF_2 reduces S_u more effectively than the primary CHF_2. From the parameters of both estimations in Table 3, the order of inhibition efficiency in terms of decreasing $S_{u0,max}$ is $CF_3 > CF_2 > CF$. The effects of intermediate fluorine species on combustion have been studied [6–8,13,15]. Takahashi et al. [15] investigated the kinetics of the high-temperature reactions of CF_3 with O and H and suggested that the most important pathways for CF_3 consumption involved $CF_3 + O \rightarrow CF_2O + F$ and $CF_3 + H \rightarrow CF_2 + HF$. Linteris et al. proposed dominant reaction pathways for decomposition of fluorine species based on the modeling results for CH_4/air flames inhibited by fluoromethanes [6] and fluoroethanes [7]. According to their results, CF_3 is consumed mostly through radical attack by H to form CF_2 and to a lesser extent by O and OH to form COF_2. CF_2 reacts with H to form CF, which is mainly consumed by reaction with O_2 to form CFO. CFO forms CO mainly through reaction with H and thermal decomposition. On the other hand, much of CHF_2 reacts with H to form CHF, most of which also reacts with H to form CH. The latter reactions play a minor role in the mechanism of inhibition. Hynes et al. [13] proposed the reaction pathways for CF_3CHFCF_3 decomposition in H_2/air flame, which is similar to that of Linteris et al. According to them, the reactions of CF_3 and CF_2 with H were significant inhibition pathways. From many of these studies it is suggested that inhibition effect in terms of decreasing S_u is $CF_3 > CF_2 > CF$, since CF_3 is the primary precursor to CF_2, which is the primary precursor to CF, and that the decomposition route through CF_2 will be more effective in inhibition than that through CHF_2. These results show qualitative agreement with our results of estimation as is listed in Table 3, although these inhibition effects of fluorine radicals cannot be directly related to the effects of molecular structure in our study.

The analytical estimation using structure–flammability relationships showed agreement to some degree between observed and predicted S_u for small alkanes and HFCs. In the present study, we have not quantified the extent of the difference in inhibition efficiency of the primary CHF_2 and the secondary CF_2, because of the limited data. In order to evaluate the corresponding parameter, more experimental data of compounds with the common substituents are required. For estimation of S_u with higher accuracy, a more sophisticated treatment based on more experimental data of various structures of HFCs is necessary.

3. Conclusions

In this study we determined the burning velocities of six types of fluoropropanes, including three pairs of structural isomers. The observed $S_{u0,max}$ of HFC-272 and HFC-263 isomers largely differed from each other. The difference is caused by the distribution of F atoms in the molecule, with $S_{u0,max}$ higher in the molecules with more distributed F atoms. Equilibrium calculations of the concentrations of chemical species in the fluoropropane flames shows that the concentrations of H and OH correlate with S_{u0}, and this suggests effectiveness of fluoric species in decreasing the concentrations of chain-carrying H and OH. For assessment and prediction of the flammability of HFCs, we have proposed a method of correlating the burning velocity with the molecular structure by

introducing simple descriptors of substituents. On the whole, agreement between the observed and predicted values of $S_{u0,max}$ was satisfactory. However, discrepancies between the results of the observation and the present prediction were noted, especially for C_2 compounds. In order to improve the techniques for their estimation, the number of tested compounds needs to be extended and to include a large variety of structures.

4. Experimental

Details of the experimental apparatus, sample preparation, and burning velocity measurements by means of the SV and SP methods have been described previously [3]. The six types of fluoropropanes were supplied from SynQuest Laboratories; the sample purities were 97.0% or higher and they were used without further purification. The HFC/air mixtures, which were prepared using the partial pressure method, were introduced into a spherical vessel with an inside diameter of 180 mm. The sample was fully mixed by a magnetically driven pump (the gas flow rate was typically 1.5 L min^{-1}) for 10 min. Ignition was accomplished with an electrical spark between electrodes placed at the center of the vessel. The duration of discharge across the gap was 0.5 ms, and the ignition energy was typically ca. 50 mJ. We measured the subsequent pressure increase due to the adiabatic expansion with an absolute pressure transducer (KYOWA PHS-10KA) and recorded with an analyzing recorder (YOKOGAWA DL750). After combustion, the final products were drawn from the vessel by a vacuum pump through a tube that was filled with soda lime to absorb HF. Sample ignition and pressure–time measurements were performed three times for each concentration at initial pressures of 600, 700, and 800 Torr. The initial temperature was ambient temperature, which was measured with a thermocouple (Type K).

We used schlieren photography to visualize the flame propagation. The photography experiments were conducted in a cylindrical vessel (inner diameter: 155 mm; length: 198 mm) with two acrylic windows for optical access. Sample preparation, ignition, pressure measurement, and treatment of combustion products in the system were the same as for the SV method. A xenon lamp was used as a light source. The schlieren images of the flame were recorded with a digital high-speed video camera (NAC MEMRECAM fx-K4) at a framing rate of 1000 Hz and saved on a PC. The time evolution of the flame radius was compared with that obtained from the pressure–time profile.

References

[1] S.G. Davis, C.K. Law, Combust. Sci. Technol. 140 (1998) 427–449.
[2] T. Jabbour, D. Clodic, ASHRAE Trans. 110 (2004) 522–533.
[3] K. Takizawa, A. Takahashi, K. Tokuhashi, S. Kondo, A. Sekiya, Combust. Flame 141 (2005) 298–307.
[4] K. Takizawa, A. Takahashi, K. Tokuhashi, S. Kondo, A. Sekiya, J. Fluorine Chem. 127 (2006) 1547–1553.
[5] G.T. Linteris, ASHRAE Trans. 111 (2006) 448–458.
[6] G.T. Linteris, L. Truett, Combust. Flame 105 (1996) 15–27.
[7] G.T. Linteris, D.R. Burgess Jr., V. Babushok, M. Zachariah, W. Tsang, P. Westmoreland, Combust. Flame 113 (1998) 164–180.
[8] B.A. Williams, D.M. L'Espérance, J.W. Fleming, Combust. Flame 120 (2000) 160–172.
[9] D.R. Burgess Jr., M.R. Zachariah, W. Tsang, P.R. Westmoreland, Prog. Energy Combust. Sci. 21 (1996) 453–529.
[10] S. Kondo, Y. Urano, K. Takizawa, A. Takahashi, K. Tokuhashi, A. Sekiya, Fire Safety J. 41 (2006) 46–56.
[11] S. Kondo, A. Takahashi, K. Tokuhashi, A. Sekiya, Y. Yamada, K. Saito, J. Fluorine Chem. 117 (2002) 47–53.
[12] S. Kondo, K. Takizawa, A. Takahashi, K. Tokuhashi, J. Hazard. Mater. A109 (2004) 13–21.
[13] R.G. Hynes, J.C. Mackie, A.R. Masri, Combust. Flame 113 (1998) 554–565.
[14] J. Berkowitz, G.B. Ellison, D. Gutman, J. Phys. Chem. 98 (1994) 2744–2765.
[15] K. Takahashi, Y. Sekiuji, Y. Yamamori, T. Inomata, K. Yokoyama, J. Phys. Chem. A 102 (1998) 8339–8348.